A framework for the behaviour of unsaturated expansive clays[1]

A. GENS AND E. E. ALONSO

Geotechnical Engineering Department, E.T.S. Ingenieros de Caminos, Gran Capitán s/n. Módulo D-2, Technical University of Catalunya, 08034 Barcelona, Spain

Received December 21, 1991

Accepted August 12, 1992

The paper presents a framework for describing the mechanical behaviour of unsaturated expansive clays. It is an extension of an existing formulation developed for unsaturated soils of low activity. The extended framework is based on the distinction within the material of a microstructural level where the basic swelling of the active minerals takes place and a macrostructural level responsible for major structural rearrangements. By adopting simple assumptions concerning the coupling between the two levels, it is possible to reproduce major features of the behaviour of unsaturated expansive clays. Some selected qualitative comparisons between model predictions and experimental results reported in the literature are presented. Despite the simplified hypotheses made, a very encouraging agreement is obtained.

Key words: capillarity, clay, model, unsaturation, suction, expansive soils.

L'article présente un cadre de référence pour décrire le comportement mécanique des argiles gonflantes non saturées. Il s'agit d'une extension d'une formulation existante pour les sols non saturés de faible activité. Le cadre de référence étendu est basé sur la distinction à l'intérieur du matériau d'un niveau de microstructure où le gonflement de base des minéraux actifs se produit, et un niveau de macrostructure responsable de réarrangements structuraux majeurs. En adoptant des hypothèses simples concernant le couplage entre les deux niveaux, il est possible de reproduire des caractéristiques majeures du comportement des argiles gonflantes non saturées. Des comparaisons qualitatives choisies entre les prédictions du modèle et les résultats expérimentaux donnés dans la littérature sont présentées. En dépit des hypothèses simplifiées utilisées, une concordance très encourageante est obtenue.

Mots clés : capillarité, argile, modèle, non saturation, succion, sols gonflants.

[Traduit par la rédaction]

Can. Geotech. J. **29**, 1013–1032 (1992)

Introduction

Unsaturated expansive clays are a type of soils that, because of their mineralogical composition, usually experience large swelling strains when wetted. If the clay is in a saturated state, large swelling strains are also observed when the soil is unloaded. These soils have also been referred to in the literature as active clays and swelling clays. Because all clays swell to some extent, in this paper they will be called expansive soils or clays, reserving the term active to the highly swelling clay minerals involved.

The behaviour of unsaturated expansive clays is closely associated with the mechanical and physicochemical phenomena occurring at particle level which are a consequence of the particular properties of the active clay minerals contained in the soil. There is a growing body of knowledge concerning those phenomena which have a direct bearing on the mechanical behaviour of this type of materials. It should not be overlooked, however, that in many cases those interactions take place in a soil structure where other factors may have a significant role in observed behaviour. Probably the most important of these factors is the negative pressures associated with the capillary water in the soil which plays its role in the interconnected pores of the clay macrostructure where water has a relatively large mobility. In contrast, physicochemical effects affect mainly the water linked to the individual clay platelets and to larger units of closely packed particles.

Until now most descriptions of unsaturated expansive soil behaviour have used an empirical approach, which has often been sufficient to tackle many problems of engineering significance. However, it is felt that there is a need to develop a more general framework that integrates the different aspects of behaviour in a consistent and unified manner. To do so, a conceptual model has been developed in an effort to provide a common framework to a variety of experimental results reported in the literature. Some benefits may be derived from such an approach. (1) It offers a consistent way of analysis and provides new criteria to interpret laboratory results and their relationships. In this way, available experimental evidence, in some cases isolated and providing apparently unrelated results, may be used in a rational way to improve our present understanding. (2) The future experimental research may be planned in a systematic way, favouring stress paths that are relevant to elucidate key questions of behaviour. (3) Basic as well as dependent parameters may be isolated and given their real significance. This opens the opportunity for a more fundamental approach to laboratory testing both from theoretical and practical viewpoints. (4) Once the framework is described mathematically and becomes a constitutive model, possibilities are open for solving boundary-value problems related to complex problems.

The well-established behaviour at full saturation is a necessary boundary condition that has to be respected by the framework developed. As shown in the paper, this constraint is properly satisfied if some basic concepts that apply to saturated soil behaviour, and specifically those concerning the application of hardening elastoplasticity, are retained.

The framework presented in this paper is an extension of a model for unsaturated soils developed by the authors (Alonso *et al.* 1987, 1990). A summary of this model is briefly presented first. The paper follows with a review of some aspects concerning soil microstructure and expansion

[1]Paper presented at the "Workshop on Stress Partitioning in Engineered Clay Barriers." May 29–31, 1991, Duke University, Durham, N.C.

Printed in Canada / Imprimé au Canada

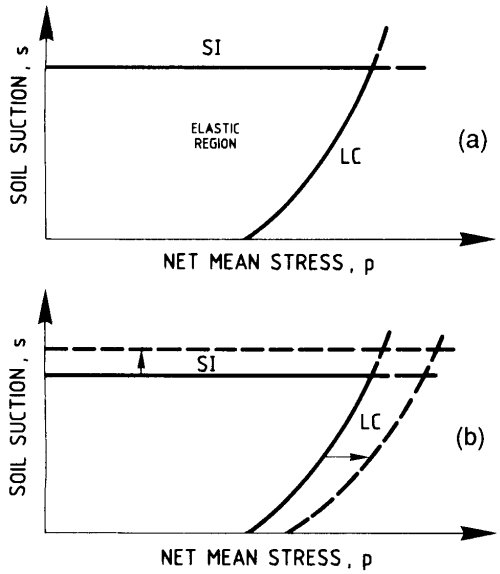

FIG. 3. (*a*) Loading–collapse (LC) and suction increase (SI) yield surfaces. (*b*) Coupling between the LC and SI yield curves.

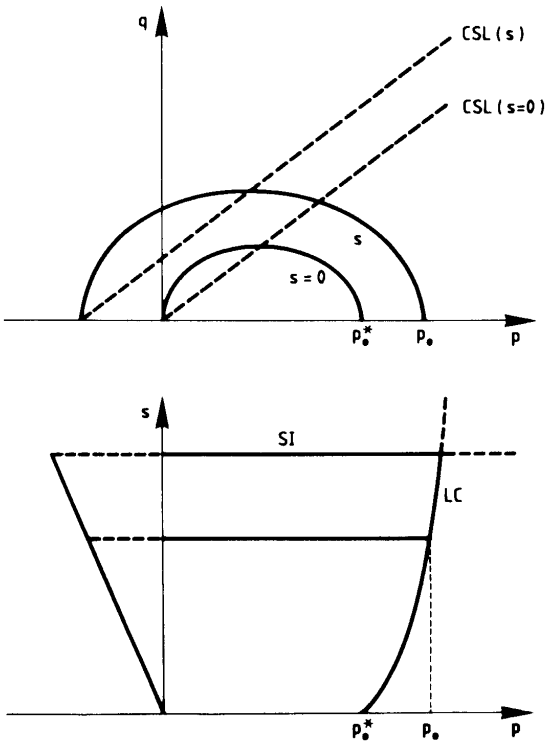

FIG. 4. Yield surface in *p*–*q*–*s* space. CSL, critical state line.

they will have a similar effect on the structure of the material as represented by the movement of the yield curve. In the case of Fig. 1, both L and C stress paths take the yield surface to the same position, and therefore the volumetric strains will be the same in this case. The hardening implied in this process is the same as that experienced by a saturated sample moving from A1 to A2. The volume change, therefore, can be estimated from the volume change that would be experienced by a saturated normally consolidated sample over the stress increment $(p_o^*)_1$ to $(p_o^*)_2$. As a consequence, the fact that the distance between the yield curves increases with the value of s implies that the volumetric stiffness under increasing applied loads also becomes higher with suction. Naturally, other stress paths combining simultaneous changes in p and s will have similar effects as long as the stress path moves outside the yield curve. To the left of the yield curve an elastic zone is postulated in which reversible deformations occur in response to suction and net total stress changes. This yield curve is called LC (loading–collapse).

To illustrate the basic consequences of the framework, an example is provided in Fig. 2. Three compression stress paths (L1, L2, and L3) and three wetting stress paths (C1, C2, and C3) are shown in Fig. 2*a*. The volume-change behaviour predicted by the framework for the loading stress paths is shown in Fig. 2*b*. Small reversible volumetric strains occur during the earlier part of the tests, but irrecoverable strains appear when the stress paths cross the LC yield curve. It can be observed that the stiffness after yield decreases as suction decreases, whereas the value of the apparent preconsolidation pressure (yield stress) increases with suction.

The predicted results of the wetting tests show the dependence of swelling–collapse behaviour on applied stress. All the samples start at the same suction, but the wetting is applied at different values of p. The saturation stress path of the first sample is contained entirely in the elastic zone, and therefore only a small swelling occurs. The sample C2 experiences an elastic swelling at first, but when it reaches the yield curve large collapse strains take place until saturation. Finally, sample C3, wetted at a higher stress, is very near the LC curve initially and therefore exhibits little swelling before collapsing. Large collapse strains are predicted for this case.

There is another source of irreversible deformations which must be taken into account in the formulation of the framework. There is evidence that suction increases beyond the maximum past suction experienced by the soil cause irreversible strains (see for instance Yong *et al.* 1971). This fact suggests the existence of the yield curve SI (suction increase) and, until more information is obtained, it will be simply assumed that this yield surface is a straight line parallel to the p-axis. Therefore, the complete framework describing the volumetric behaviour of an unsaturated soil of low activity will be represented by the two yield surfaces SI and LC bounding the elastic region (Fig. 3*a*). The irreversible strains that occur when crossing the SI surface must indicate a change in the soil structure that should affect the position of the LC surface. Tests reported by Josa *et al.* (1987) and Vicol (1990) have shown that a drying–wetting cycle causes an increase of the apparent preconsolidation pressure of the saturated soil which implies a movement to the right of the LC surface as indicated in Fig. 3*b*. Because the hardening associated with the movement of the LC yield surface is assumed to depend on plastic volumetric strains only, its

position can be related to the void ratio of the soil. Denser soil packings result in LC yield surfaces located farther to the right in the (p, s) space.

The formulation has been extended to triaxial stress space by incorporating a third stress parameter $q(= (\sigma_1 - \sigma_3))$ and adopting as starting point a critical state type model for the saturated condition. For $s = 0$ (saturated soil) the yield surface can be, for instance, the ellipse of the modified Cam-clay model. This can be generalized by considering different ellipses for each particular suction value (Fig. 4). The yield stress p_0 varies in accordance with the shape of the LC yield surface in the (p, s) plane. The increase in strength with suction is accounted for by allowing the critical state line (CSL) to vary with the value of suction. For simplicity, it is assumed that the slope of the critical state lines remains constant, although other choices can be easily implemented. With respect to the SI surface it is assumed that it rises vertically, i.e., no explicit dependence on q is postulated. A three-dimensional view of the complete yield surface for a given value of plastic volumetric strain is depicted in Fig. 5. It is recognized that the modified Cam-clay model does not provide an accurate description of the detailed features of real soil behaviour and that more sophisticated models are required if a more complete reproduction of actual behaviour is sought. However, in this case the simpler choice is considered adequate in order that the complexity of the saturated model should not interfere with the main objective of incorporating the basic features of unsaturated soil behaviour in a unified framework.

A mathematical formulation of the framework has been presented in Gens *et al.* (1989) and Alonso *et al.* (1990). Although a mathematical model is necessary to obtain quantitative predictions and to ensure the consistency of the formulation, very useful qualitative predictions concerning the main features of unsaturated soil behaviour can be derived directly from the conceptual model outlined above. As shown in Alonso *et al.* (1987, 1990), the framework is able to predict many of the basic patterns of behaviour which have been observed in unsaturated soils.

Extension of the framework to expansive soils: conceptual basis

The framework described in the previous section is not able to reproduce the large swelling strains exhibited by expansive soils. The formulation allows only for small reversible swelling in the elastic zone, whereas expansive clays experience large volumetric changes that can be largely irreversible. Moreover, a basic fact in the behaviour of unsaturated expansive soils is the central role played by the various phenomena occurring at particle level. To develop a model consistent with present understanding of these basic phenomena, it appears necessary to incorporate explicitly the microstructural effects in the formulation. In fact, it is likely that the key element in the framework is to define satisfactorily the effects of particle-level phenomena on the overall behaviour of the material. To do this, it is necessary to take into account some fundamental aspects of soil microstructure.

Based on scanning electron microscopy (SEM) observations reported by Collins and McGown (1974), McGown and Collins (1975), and Collins (1984), it is possible to envisage, for expansive soils, the fabric types shown in Figs. 6*a* and 6*b*, although, naturally, intermediate types are also possible. These structural arrangements are made up by three basic microfabric features: elementary particle arrangements or quasi-crystals (Fig. 6*c*), particle assemblages, and pore spaces. In fabric *a* the particle assemblages are formed by arrays of elementary particle arrangements, and they are described as matrices. The pore space is made up of intra-matrix pores existing between elementary particle arrangements. In fabric *b* the elementary particle arrangements join together to make aggregates resulting in a three-dimensional structure of a granular type. Both inter- and intra-aggregate pore spaces exist. In both types of macrofabric there is a further level of void space, the intraelement pores separating the clay platelets in the elementary particle arrangements (Fig. 6*c*). If the clay minerals constituting the elementary particle arrangements belong to expansive types, microfabrics *a* and *b* will result in highly swelling soils, although collapse phenomena can also occur in some circumstances, especially in the case of microfabric type *b*.

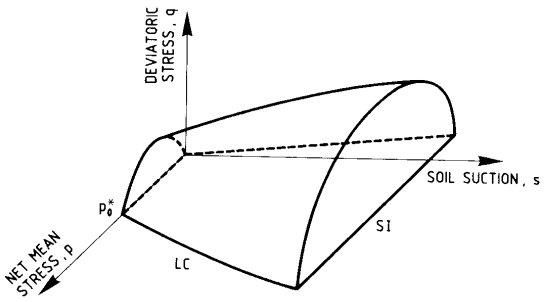

FIG. 5. Three-dimensional view of the yield surface.

The extended framework will be based on considering two levels of soil structure: (*i*) a microstructural level that corresponds to the active clay minerals and their vicinity, where physicochemical interaction phenomena predominate; it is likely that this level can be considered saturated even when the soil as a whole is in an unsaturated state; and (*ii*) a macrostructural level that accounts for the larger scale structure of the soil.

The deformation of the microstructural level will be controlled by physicochemical interactions at particle level and will be assumed independent of macrostructural effects. The description of the behaviour of the microstructural level should therefore be based on theories concerning the clay–water–cation interaction at platelet scale. This will be discussed further later in the paper. On the other hand, the deformations due to loading and collapse will have major effects on the macrostructural level and can be described by the framework summarized earlier. However, a basic point of the extended framework is that the deformation of the microstructure is able to affect the macrostructural level.

The phenomena affecting the microstructural level will occur in the vicinity of the individual clay platelets, and therefore this level can be identified with the elementary particle arrangements constituted by the clay platelets and the intraelement pores. The macrostructural level in the microfabric type *a* of Fig. 6 will refer to the overall structure of the elementary particle arrangements which includes the

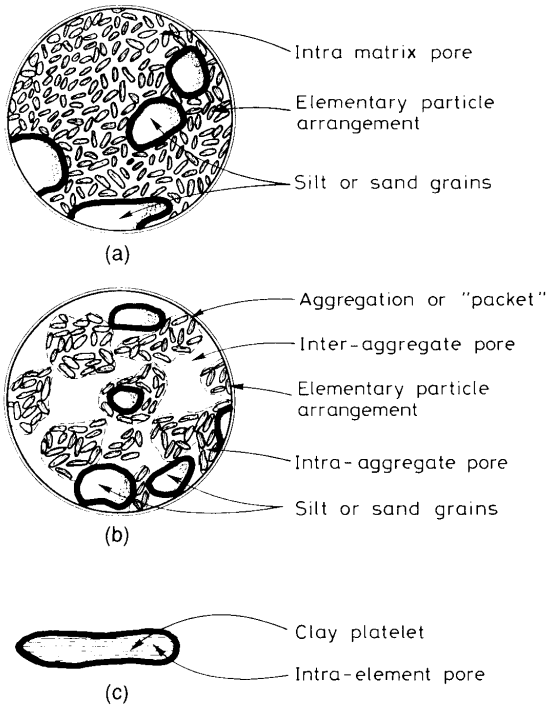

FIG. 6. Fabric types. (*a*) Clay matrix predominantly constituted by elementary particle arrangements of clay platelets. (*b*) Microfabric of a clay predominantly made up of aggregations of elementary particle arrangements. (*c*) Elementary particle arrangement in a parallel configuration.

intramatrix pores. In microfabric type *b* the macrostructural level involves the ensemble of particles and (or) aggregates together with the interaggregate pores. In this case the intra-aggregate pores are not explicitly considered, as they would require a third level of structure, with the consequent increase of complexity of the framework. Because the effect of intra-aggregate voids in this case is small compared with the effect of the deformation of interaggregate pores, they can be neglected.

The occurrence of microfabric of type *b* is very widespread both in natural and compacted soils. Pusch (1970, 1973), Delage *et al.* (1982), Delage and Lefebvre (1984), and Lapierre *et al.* (1990) have reported that this kind of fabric is observed in natural clays, usually of a sensitive type. Compacted soils, generally on the dry side, also exhibit a similar type of structural arrangement (see, for instance, Croney *et al.* 1958; Sridharan *et al.* 1971; Smart 1973; Yong and Sheeran 1973; Juang and Holtz 1986). It is interesting to note that samples resedimented in the laboratory also appear to adopt the same type of microfabric (Lapierre *et al.* 1990).

In the case of highly active clays it has been reported that the initial microstructure of compacted granulated bentonite powders exhibits the same kind of arrangement, namely aggregates of clay particles leaving relatively large interaggregate voids (Pusch 1982). This is confirmed by the porosimetry studies reported by Atabek *et al.* (1991) and reproduced in Fig. 7. The bimodal pore-size distribution is clearly apparent for all values of moulding water content. A further example of this type of microfabric is provided by Wan *et al.* (1990) concerning the structure of sand–bentonite mixtures. They show that aggregates containing sand particles form during the mixing and compaction operations required for sample preparation, the size of the aggregations increasing with mixing moisture content. In addition, they draw attention to the important influence of initial structure on subsequent behaviour. Microfabric type *b* also plays a central role in the conceptual model proposed by Brackley (1975*b*) to describe the behaviour of swelling clays.

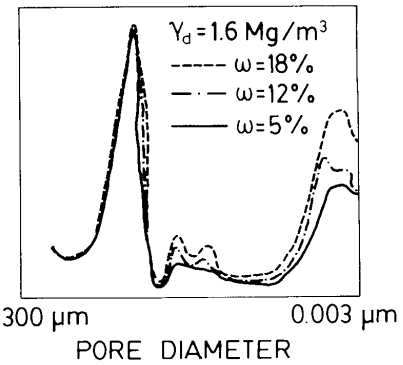

FIG. 7. Pore-size distribution in compacted FoCa clay (after Atabek *et al.* 1991). *w*, water content.

Porosimetry studies have shown that in most soils external loads affect mainly the macrostructural voids, leaving the microstructural pore space largely unchanged. This has been observed again in natural clays (Delage and Lefebvre 1982; Lapierre *et al.* 1990) and in compacted soils (Juang and Holtz 1986). Therefore, in inert materials the microstructural level does not experience significant variations and can be neglected. However, in active clays the interparticle separation can vary widely in response to external actions of various types (load, chemical phenomena, suction changes), and the associated deformations are a major feature of their mechanical behaviour.

Formulation of the extended framework

The aim of this paper is to present a general framework that encompasses both types of soil microfabric. In soils with a microfabric type *b* the adequate description of the macrostructural behaviour and the relationship between the two structural levels will be crucial for a satisfactory modelling of their behaviour. On the other hand, in soils with microfabric type *a* the most critical element in the model will be the good description of the behaviour of the microstructural level, with the macrostructural level playing a lesser role. Therefore, to achieve sufficient generality, the formulation of the extended framework should include definition of (*i*) behaviour of the macrostructural level, (*ii*) behaviour of the microstructural level, and (*iii*) coupling between the two structural levels.

The behaviour of the macrostructural level is assumed to be described by the framework of unsaturated soil behaviour presented above. In contrast, the modelling of the behaviour

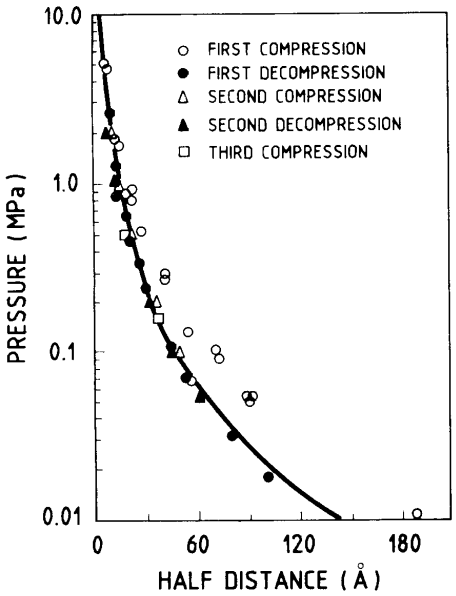

FIG. 8. Relationship between interparticle spacing and swelling pressure for montmorillonite (after Warkentin *et al.* 1957).

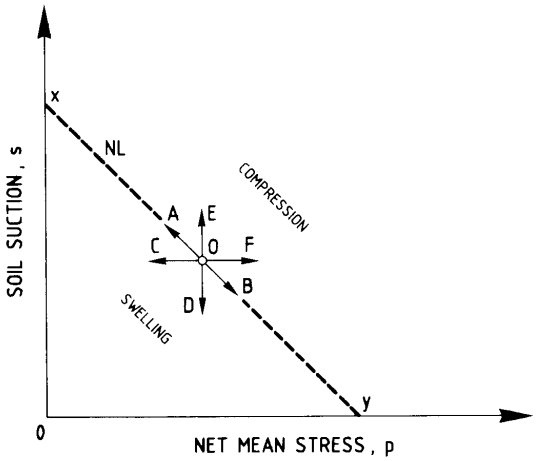

FIG. 9. Microstructural behaviour. Neutral loading line (NL) separating compression from swelling regions.

of the microstructural level must address the basic interactions occurring at particle level.

In general, the microstructural level will have a predominant influence on behaviour in soils of high density and high activity, whereas the macrostructural level will play a more important role when the soil has a more open structure. In this context, it is interesting to note that the results of Atabek *et al.* (1991) for montmorillonite powder compacted at a dry density of 1.6 Mg/m^3 (Fig. 7) show a clear bimodal pore structure, suggesting a well-developed macrostructural level at this density value. Only at dry densities of 1.84 and 1.95 Mg/m^3 do the bigger pores tend to disappear, and the structure becomes largely matrix dominated.

Basic mechanisms of soil expansion

The most widely used approach to relate clay compressibility to basic particle–water–cation interaction is the use of the Gouy–Chapman double-layer theory (Gouy 1910, 1917; Chapman 1913). According to this theory, the interacting force between two double layers depends on the ion concentration at the midplane between two adjacent particles and is given by the equivalent osmotic pressure in that plane (i.e., Bolt 1956). One advantage of this approach is the fact that the effects of factors such as electrolyte concentration, dielectric constant, cation valence, and temperature can be deduced from the theory.

This approach has been used to predict volume change of expansive clay minerals with a fair degree of success. For instance, good agreement is reported between the measured and theoretical pressure – interparticle distance relationships for a less than 0.2 μm fraction of montmorillonite in 10^{-4} M NaCl (Fig. 8). The agreement is not as good at higher electrolyte concentrations or for larger size clay minerals such as illite (Bolt 1956). However, the trends for the effects of cation valence and electrolyte concentrations are reproduced satisfactorily. Other successful applications of double-layer concepts are reported by Olson and Mesri (1970), Mitchell (1973), Sridharan and Rao (1973), Callaghan and Ottewill (1974), Sridharan and Jayadeva (1982), and Jayadeva and Sridharan (1982). More recently, Madsen and Müller-Vonmoos (1985) report good agreement between the swelling pressures computed from double-layer theory and those measured in tests on 19 core samples of intact opalinum shale.

It has been always recognized that the predictions of double-layer theory cannot be exact because the parallel clay-particle arrangement is too simple to represent real soil structures (Yong *et al.* 1984). There are also other factors, such as the effect of ion size, anion adsorption, and the existence of attractive forces, that are not considered in the theory. In response to this, modified theories have been proposed to overcome some of those shortcomings such as the anisotropic hypernetted chain model developed by Kjellander and co-workers (Kjellander 1991), which better reproduces the observed swelling if bivalent cations are present, and the particle interaction model proposed by Yong *et al.* (1984), which takes into account the various modes of fabric interaction.

Alternative approaches have been proposed. For instance, Low and Margheim (1979) and Low (1980, 1991) contend that double-layer theory does not explain satisfactorily the experimental results of montmorillonite swelling. They believe that double layers are poorly developed and that the basic mechanism for swelling potential is the modification of the interlayer water potential as a result of its interaction with the adjacent layer surface. They have found that an exponential empirical relationship that relates swelling pressure and interlayer distance is not affected by the nature of exchangeable cations or the charge density of the particles and is applicable to a wide range of materials. Pusch (1982) also reports a large discrepancy between experimental data and relationships derived theoretically from double-layer theory for a highly compacted Na-bentonite. The difference is attributed to the fact that at high densities double layers are not developed or are only partly developed.

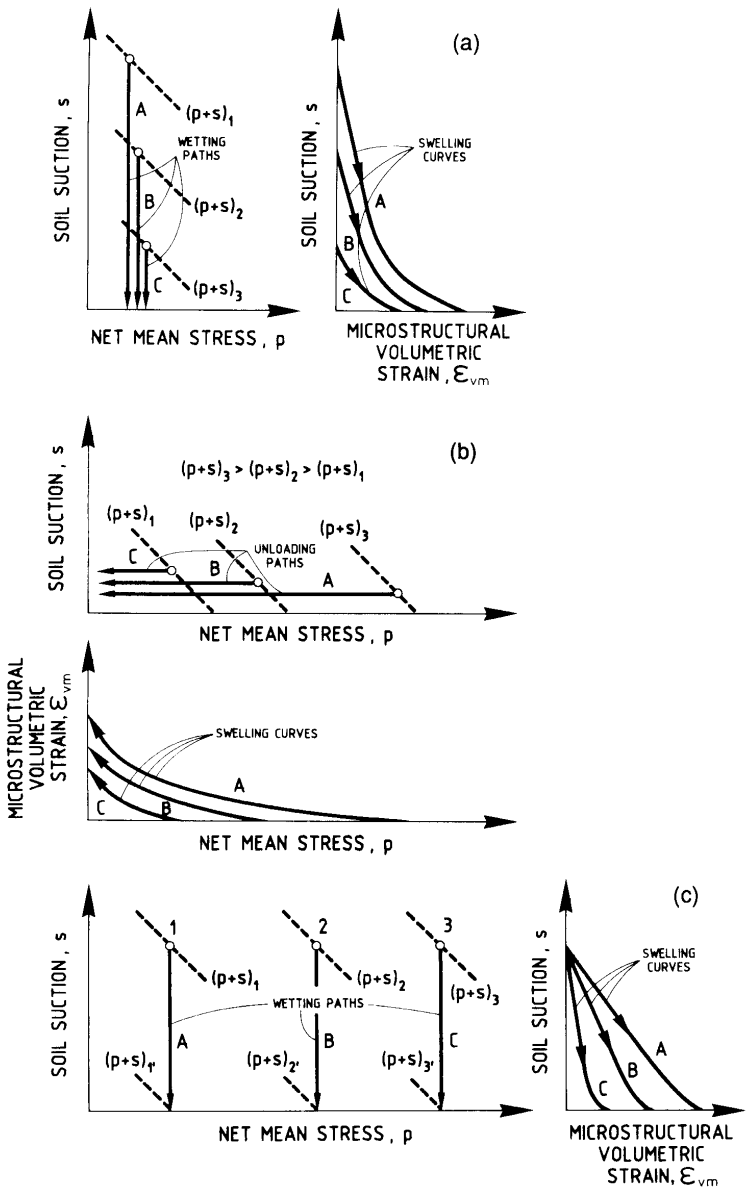

FIG. 10. Behaviour of the microstructural level. (*a*) Dependence of microstructural swelling strains on suction variation. (*b*) Dependence of microstructural swelling strains on applied net stress variation. (*c*) Influence of applied net stress on microstructural expansion.

Finally, it should be recognized that the real picture of the interactions at particle level may be in fact more complex and that, in addition to the osmotic and hydration effects mentioned above, the direct mechanical effect of water in tension may contribute significantly to the volume-change behaviour (Baveye *et al.* 1991; Tessier 1991).

An important point concerning the microstructural deformations is whether they are reversible or not. In principle the basic interaction phenomena responsible for the microstructural volume changes appear to be basically reversible. However, irreversible strains are measured in some tests. For instance, in the test on Na-montmorillonite reported by Warkentin *et al.* (1957) irreversible deformations occur during first loading, although they are quite small. Somewhat large irreversible strains are observed in the tests on Ca-montmorillonite. This irreversibility is attributed to an

initial lack of particle parallelism, which disappears upon first loading. Concerning the same point, Branson and Newman (1983), Ormerod and Newman (1983), and Kraehenbuehl *et al.* (1987) report only a slight hysteresis in the water content – suction curves of illite and montmorillonite. Again, the irreversibility involved is small and it is attributed to a structural ageing effect of drying in which interlamellar volume increases at the expense of external surfaces.

Behaviour of the microstructural level

It is evident that the question of the correct description of the behaviour of the microstructural level is not settled. For the formulation of the framework it will be assumed that there exists a model which allows the calculation of the volume changes occurring at particle level. As a first approximation the double-layer theory could be used, although other alternative approaches such as the empirical relationship proposed by Low (1980) may be adopted if desired. The formulation of the framework is independent of the particular microstructural theory adopted.

To keep within the basic approach of simplicity, it will be assumed that microstructural deformations are reversible and independent of the macrostructure. Possible irreversibility effects can be introduced, if required, at a later stage of the development of the framework. It is important to note that, as the microstructural level is likely to remain saturated, the effects of changes of suction and of external applied stress, in accordance with the principle of effective stresses, are likely to be equivalent. A series of elegant tests performed on a matrix-dominated mixture of sodium bentonite and silica sand reported by Graham *et al.* (1992) gives strong support to this assumption. Hence, the microstructural approach adopted should yield an equation of this type:

$$[1] \quad \epsilon_m = f(s + p, \text{ other factors})$$

where ϵ_m are the microstructural strains. This is also consistent with the tenets of double-layer theory. In this qualitative approach only microstructural volumetric strains ϵ_{vm} will be considered.

In a (p, s) space (Fig. 9), the stress trajectories OA and OB correspond to neutral loading paths. As the value of $(s + p)$ remains constant, no microstructural deformations takes place. Therefore the neutral loading line X–Y (NL) separates stress paths, causing swelling from stress paths, causing compression. The reductions in suction or pressure (stress paths OC–OD) will lead to microstructural expansion, whereas an increase in suction or pressure (stress paths OE–OF) will bring about microstructural compression. It should be pointed out that depending on the microstructural theory adopted a different inclination of the neutral loading line could perhaps be obtained in some suction–stress regions. However, in the rest of the paper a 45° slope of the neutral line will be assumed throughout the (p, s) space.

Independently of the model adopted in the description of the microstructural behaviour, there is agreement on the general trends regarding the effects of applied stress and suction on swelling. These basic features of behaviour are illustrated schematically in Fig. 10. Figure 10*a* shows that, at a constant applied stress, a reduction in suction from a higher value results in a larger expansion. The rate of increase of swelling strains with suction becomes larger when the lower values of suction are reached. A similar consideration applies to reductions of applied stresses at constant suction (Fig. 10*b*). Existing microstructural theories also predict that the microstructural expansion due to a suction reduction will be smaller the larger the value of the applied stress (Fig. 10*c*).

Coupling between the two structural levels

Although the microstructural deformation is considered independent of the macrostructure, the reverse is not true. If a specimen initially at point A (Fig. 11*a*) is taken, via a suction reduction, to point B, microstructural swelling will take place. This swelling will affect the soil skeleton, increasing its macrostructural void ratio. This plastic volume change leads in turn to a movement of the LC to the left (a softening in hardening plasticity terms) in response to the new structural arrangement. It is quite possible that the effects of a microstructural volume change affect the macrostructure in a different way from that due to purely macrostructural phenomena such as loading or collapse. However, as a first approximation, it will be considered that the macrostructural void ratio changes have the same effect irrespective of their origin. If the suction reduction is continued, the stress path will tend towards C and further movement of the LC curve towards the origin will ensue. However, it is assumed that if the stress path reverses from point B towards A, no irreversible macrostructural strains are induced and, therefore, the LC curve remains unchanged. Therefore the neutral line plays a role similar to that of a yield locus. This is a simplifying assumption that is likely to be only approximate and may require modification when more complex versions of the framework are developed. The SI surface has been omitted from Fig. 11*a* for clarity. If necessary, it can be introduced in the framework without requiring any specific conceptual change. It is recognized that the existence of particle bonding could also contribute significantly to the irreversibility of strains caused by microstructural swelling. This factor, however, is not explicitly considered in the framework.

A final postulate of the framework refers to the relationship between the microstructural expansion ϵ_{vm} and the irreversible macrostructural swelling it causes, ϵ^p_{vM}. It is assumed that this relationship depends on the value of p/p_o in a way such as that depicted in Fig. 11*b*, where p is the currrent value of applied net stress, and p_o is the apparent preconsolidation stress of a soil at the current value of suction. A value of $p/p_o = 1$ corresponds to a very open macrostructure, as the soil is in a potentially collapsible situation. Decreasing values of p/p_o imply increasingly denser packings of the macrostructure. It is therefore reasonable to assume that the proportion of macrostructural strains caused by the expansion of the microstructure increases as the value of p/p_o reduces. In the limiting case of $p/p_o = 1$, it is assumed that $\epsilon^p_{vm}/\epsilon_{vm} = 0$.

The effect of this hypothesis is illustrated in Fig. 12. It is assumed that samples A and B are at the same stress–suction point, but they have different initial LC yield curves, LC_{A_i} and LC_{B_i}. As shown in the right-hand part of the figure, sample B will swell more than sample A upon saturation. Although, according to the framework, the microstructural swelling will be the same in both samples, the irreversible macrostructural strains induced by the microstructural expansion will be higher for sample B because the distance from the stress point to its LC yield curve is larger than for sample A. Comparing the results of tests A and A′, the

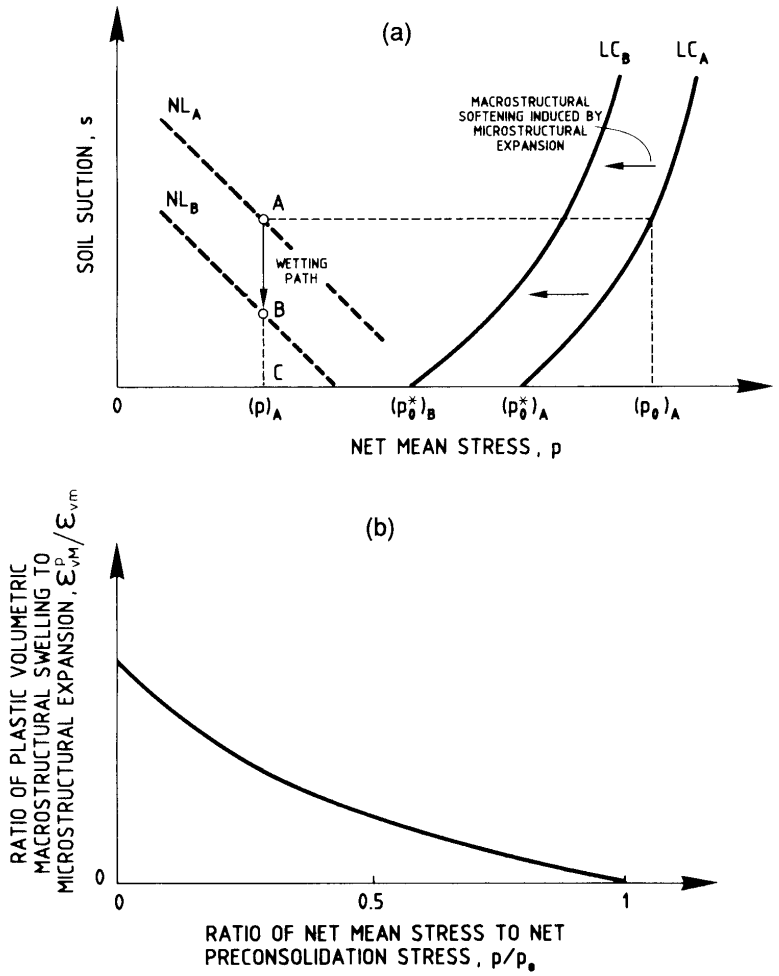

FIG. 11. (*a*) Coupling between microstructural deformation and macrostructural LC yield curve. (*b*) Dependence of the ratio between irreversible volumetric macrostructural deformation and microstructural swelling on the value of p/p_0.

framework will predict that the swelling due to saturation will be far higher in the case of sample A. The origin of the difference is twofold. Firstly, the microstructural swelling is larger in sample A because of the lower applied stress but, in addition, the macrostructural strains induced by microstructural swelling will also be higher in sample A because of its greater distance to the corresponding LC yield curve. The same considerations apply to the comparison between samples B and B′. It should be stressed that the neutral loading lines and the LC yield curves of Figs. 11 and 12 refer to different levels of structure. They are represented in the same plot as an aid to understanding, but it would be conceptually more rigorous if they were plotted in different spaces.

Features of expansive soil behaviour and model application

As indicated above, the development of the framework has been based on the combination of an existing model for nonexpansive soils with the behaviour of active clay minerals in simple configurations with the purpose of describing the basic features of real expansive soil behaviour. The validity of the framework, therefore, should be tested by comparing its qualitative predictions with reported results of tests on expansive soils.

It should be pointed out that most of the tests described in the literature correspond to oedometer conditions with no measurement of horizontal confining stresses. The stress state is therefore not fully known, and this introduces some difficulties in the interpretation of results and the comparison, even if qualitative, with model predictions. However, general trends of behaviour are conveniently displayed in those tests, and a suitable model of constitutive framework should be able to reproduce the significant features observed in them. The comparisons offered subsequently have been made having this comment in mind.

An added difficulty to perform the comparisons comes from the type of stress paths imposed to the samples. In

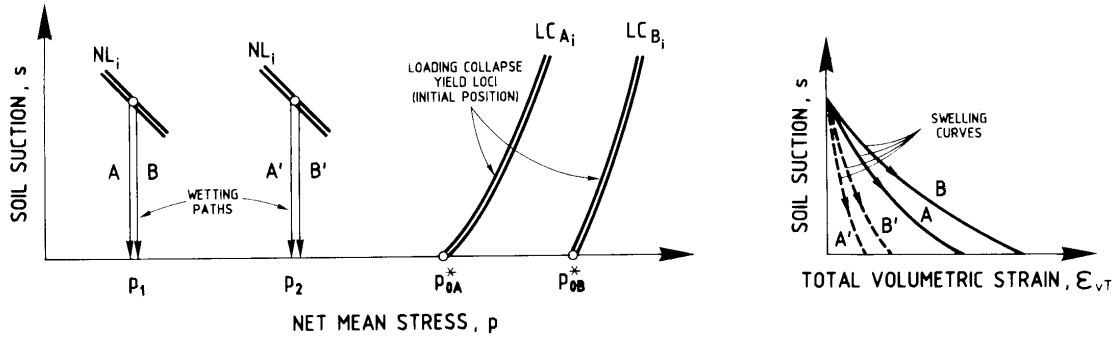

FIG. 12. Effect of the relative position of the LC yield curve on the magnitude of swelling.

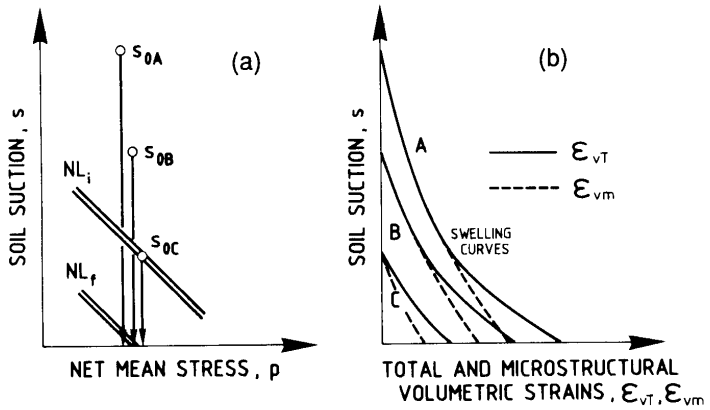

FIG. 13. Wetting from different initial suctions at constant confining stress. (*a*) Stress paths in (p, s) stress space. (*b*) Total and microstructural volumetric deformations.

general terms most of the papers reviewed try to identify the "swelling potential" of the soil. This term refers either to the swelling volumetric deformation or to the swelling pressure measured along wetting paths. The specific paths imposed usually involve an ever-decreasing value of the suction applied and different sequences of vertical load. As a consequence, stress and particularly suction reversals are uncommon. Reversible and irreversible components of deformation, which are a key concept in the framework developed, cannot therefore be properly identified in a direct manner in most cases. Nevertheless, the review performed has provided a set of interesting results that will be used in a first evaluation of the model.

Swelling deformation

A commonly performed experiment is the swell under load test. Figure 13*a* indicates the type of stress paths imposed to the samples: suction is reduced from its initial value at a constant p stress. In Fig. 13*a* the paths plotted are supposed to cross a neutral line initially located at some position N L_i. The three paths indicated take this yield locus to the final position N L_f. The model predictions are qualitatively indicated in Fig. 13*b*. The initial portion of paths of samples A and B induce reversible swelling of the microstructure, ϵ_{vm}. Plastic components are added when N L_i is reached, as indicated in Fig. 13*b*. Tests of this kind have been reported by many authors. A set of interesting results were published by Kassiff *et al.* (1973). They were obtained in an oedometer cell in which suction was controlled by an osmotic technique developed by the authors. Samples of a high-plasticity clay (w_L = 72%; I_P = 48%) were compacted at a common dry density (γ_d = 14.7 kN/m^3) and varying initial water contents. They were then brought to equilibrium under different suctions and various vertical loads. Some of the originally published swelling data for σ_v = 19.6 kPa have been replotted in Fig. 14 in terms of suction versus volumetric swelling. Total final swelling is strongly dependent on the original water content (or original suction). This is a result consistent with the developed framework. In addition (note the log scale for suction), the first stages in suction reduction induce small swelling strains if compared with the final stages. Swelling along a suction-reduction path takes place at an increasing rate. This is also consistent with the expected microstructural swelling behaviour and the theories accepted as a suitable reference for this part of the framework.

If the final total swelling for several applied stresses and initial water contents are compared, Fig. 15 is obtained. The type of stress paths followed in these tests is qualitatively indicated in Fig. 16*a* for two initial water contents (w_{o1} and w_{o2}) and three applied stresses (p_1, p_2, p_3). The swelling deformations predicted by the model have been plotted in

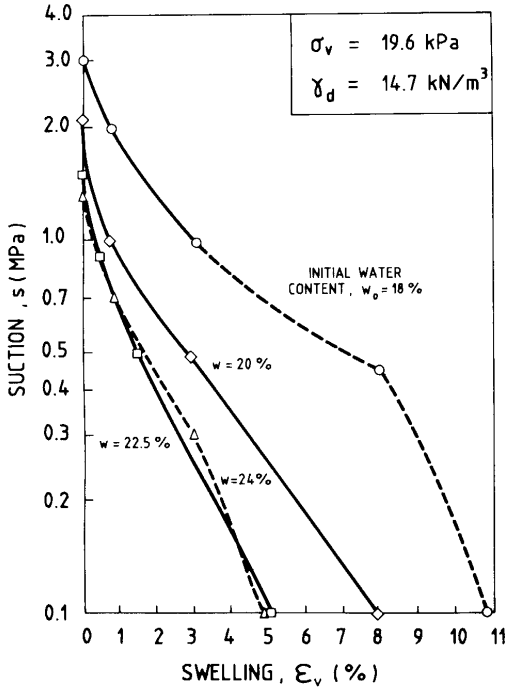

FIG. 14. Oedometer swelling results on samples compacted at the same dry density and varying initial water contents (from data published by Kassiff *et al.* 1973).

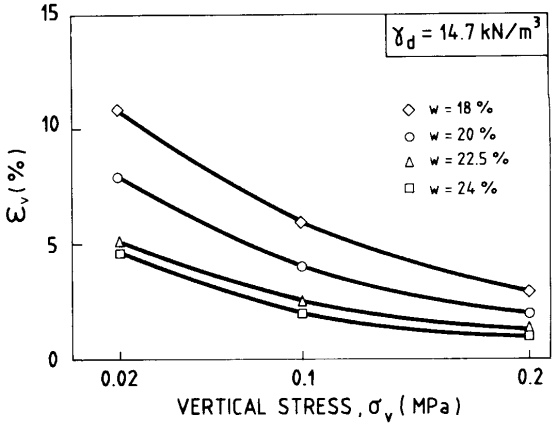

FIG. 15. Maximum swelling strain for varying applied vertical stress and initial water content obtained in the oedometer on samples compacted at the same dry density (from data published by Kassiff *et al.* 1973).

Fig. 16*b*. The reduction in volumetric deformation with applied stress has two origins: (*i*) the microstructural swelling ϵ_{vm} which varies inversely with the intensity of the applied $(p + s)$ effective stress; $(p + s)$ increases from sample 1 to sample 3 in Fig. 16*b*; and (*ii*) the plastic macrostructural swelling ϵ^p_{vM} controlled by the position of the initial neutral line N L_i and by the distance of the applied p stress to the current yield stress (not represented in the figure) for the particular suction imposed. For these reasons ϵ^p_{vM} decreases also from sample 1 (lower confining stress) to sample 3 (higher confining stress).

For a given void ratio, swelling strain is therefore controlled by applied stress (in an inverse relationship) and initial suction (in a direct relationship). However, as clearly identified by Brackley (1973), swelling strain is also dependent on original void ratio (Fig. 17). Figure 17 corresponds to the free swell obtained, under a token load of 1 kPa, in compacted samples of a weathered norite (w_L = 89%; I_P = 57%). For a given constant initial water content, swelling strain increases with decreasing void ratio (increasing dry density). This result is conveniently discussed, within the framework described before, with the aid of Fig. 18. Consider two samples, 1 and 2, at different initial void ratios e_1 and e_2 ($e_1 > e_2$) and subjected to a common initial stress state given by load p and suction $s = s_o$. The positions of the loading collapse yield curves for these two samples have been indicated (LC_1 and LC_2). The distance, in terms of p, between the initial stress state and the yield stresses p_{o1} and p_{o2} is larger for sample 2 than for sample 1. As a result, the wetting path indicated in Fig. 18*a* for both samples will induce a larger plastic strain in sample 2 (ϵ^p_{vM2}) than in sample 1 (ϵ^p_{vM1}) (Fig. 18*b*). Under different applied p stresses and a common initial suction the predicted plastic macrostructural volumetric strains have been indicated in Fig. 18*b*. This is a direct consequence of the assumed variation of ϵ_{vM} with the ratio p/p_o (Fig. 18*c*) which is one of the fundamental hypotheses of the framework proposed.

The test results presented until now have not allowed the direct identification of the reversible and irreversible components of swelling deformation. To do this, it is necessary to perform suction-controlled tests involving wetting–drying cycles. Such tests were carried out by Chu and Mou (1973) on dynamically compacted samples of two clays of high plasticity (w_L = 62.5–73.5%; I_P = 37.2–45.8%). Samples were compacted to an initial dry density and water content (γ_d = 16.4–16.5 kN/m^3; w_o = 20.2 = 20.4%) close to the optimum values obtained in modified Proctor tests. Their initial degrees of saturation were S_{ro} = 0.876 and 0.898. Samples A-1 and A-2 in Fig. 19 were subjected first to a wetting path under a surcharge pressure of 7 kPa, and then a number of drying–wetting cycles were applied. The results show that a significant part of the observed swelling is irrecoverable (plastic). The reversible part of the swelling strain is relatively small in this case.

These results are interpreted in Fig. 20. The initial state of the sample is given by the yield curves N L_i and LC_i. The initial stress point 1 moves to point 2 when suction is reduced to zero. The yield locus (N L_i) is dragged along path 1 to 2 down to its final position N L_f. The plastic swelling strains induced also displace LC_i towards its final position LC_f. A subsequent drying (2 to 3) induces only reversible strains (ϵ_{vm}). Figure 20*b* shows that the model prediction for swelling strains corresponds with Fig. 19. Note also that the successive wetting–drying cycles (Fig. 19) induce an accumulation of swelling strains, a behaviour not covered by the model in its present form.

Tests reported by Pousada (1984) allow the examination of the dependence of each deformation component with applied stress. Pousada (1984) performed cyclic suction-controlled oedometer tests on a compacted expansive clay

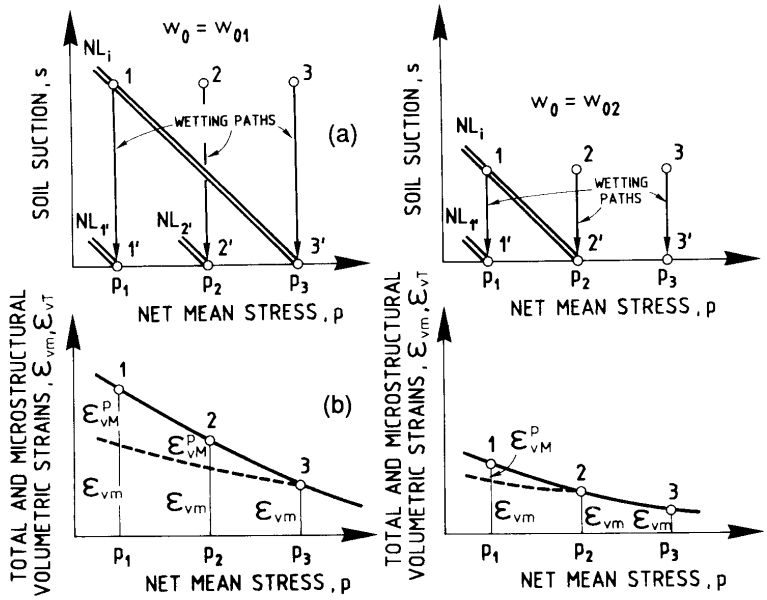

FIG. 16. Wetting from two different initial suctions (w_{01} and w_{02}) at different confining p stress. (a) Stress paths in (p, s) stress space. (b) Total and microstructural volumetric deformations.

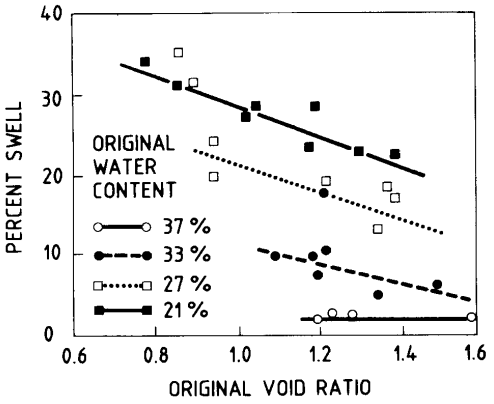

FIG. 17. Free swell as a function of original moisture content and void ratio (after Brackley 1973).

from Madrid under different vertical applied stresses. The variation of reversible (ϵ_{vm}) and irreversible (ϵ^p_{vM}) strains with applied pressure are shown in Fig. 21. It can be seen that both components decrease as the vertical stress increases, as postulated in the proposed model. It is interesting to note that in this case reversible strains are more predominant than in the Chu and Mou (1973) case, probably reflecting a difference in structure that results in a different degree of macrostructure–microstructure coupling.

Swelling pressure

Swelling pressure is an alternative measure of swelling potential favoured by many authors because it seems to be controlled essentially by initial density only. In unsaturated soils the swelling pressure may be defined as the external load that prevents any volume change when the sample is wetted. Unfortunately, it is widely recognized that this load is highly dependent on the particular stress path followed by the sample. This situation has led to several definitions of swelling pressure, as illustrated in Justo *et al.* (1984) and Sridharan *et al.* (1986). This stress-path dependency and the explanation offered by the developed framework will be discussed later.

Consider now one of the possibilities. Suction is reduced and, at the same time, the load acting on the sample is continuously modified so as to prevent any volumetric deformation. The process is conveniently represented in the usual (p, s) stress space (Fig. 22). Three samples A, B, and C at the same void ratio and different initial suctions will be wetted at constant volume. Consider first the case in which the LC yield surface is not crossed by the stress paths (LC is assumed to be located to the right along the p axis). When sample A experiences a swelling tendency as a response to suction decrease (Δs), a pressure increment Δp has to develop to maintain a constant volume. If the mechanism of volume change would be solely controlled by the microstructure the stress path $\epsilon_{vm} = \epsilon_{vT} = 0$ would proceed along the neutral line as indicated by the broken line in Fig. 22. However, the increments in p and s which impose this path will also deform the macrostructure. It is known that in regions of relatively high suction the soil structure reacts rigidly against suction changes. Changes in total stress are probably more able to deform the soil. This is the case of point A in Fig. 22. In other words, in the vicinity of point A the modulus of soil stiffness against p loading is larger than the corresponding modulus for suction changes, always in terms of macrostructural deformations. If this is the case the real swelling path will follow the solid line plotted through A.

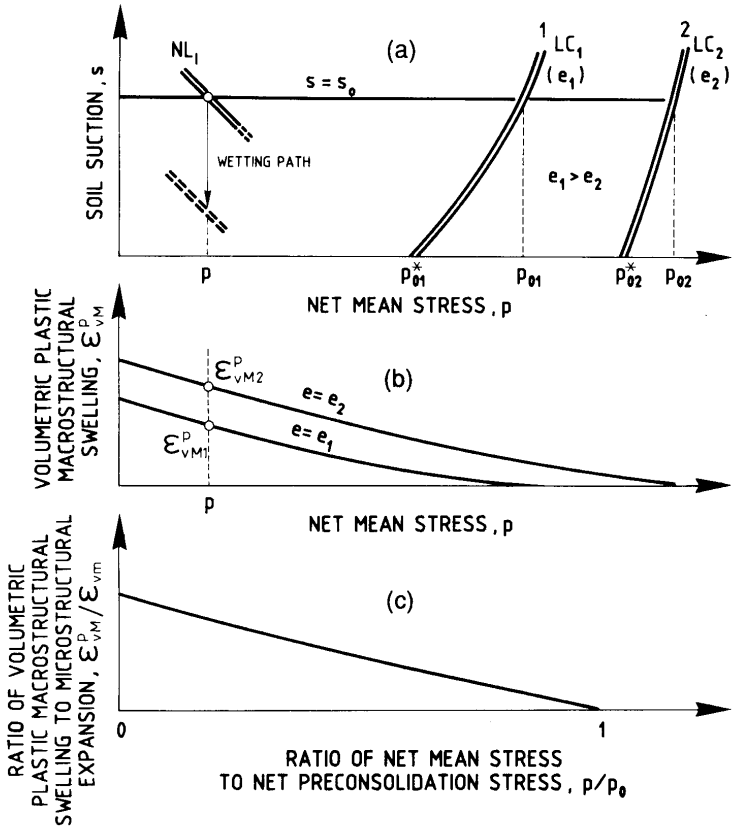

FIG. 18. Swelling strains at various confining p stresses and two different void ratios (e_1 and e_2). (a) Stress paths. (b) Plastic volumetric strains. (c) Ratio of plastic volumetric macrostructural swelling to microstructural expansion.

When suction decreases and the soil approaches saturation the soil stiffnesses against load and suction changes will tend towards similar values. Progressively the principle of effective stresses will hold and the zero volume stress path will follow the neutral line inclination down to $s = 0$. In this way swelling pressures such as p_{sA}, p_{sB}, or p_{sC} will be recorded for the three samples represented.

Stress paths of an unsaturated expansive clay (w_L = 55%; I_P = 35%) at constant volume have been published by Blight (1965) and are reproduced in Fig. 23. The trends indicated above can be identified in these interesting results. The range of applied suction (0–210 kPa) is, however, small for an expansive clay, and it should be recognized that Fig. 23 offers only a limited picture of the full stress paths experienced in practice by unsaturated expansive clays in the process of constant volume swelling. A much wider range of suction variation is provided by the tests of montmorillonitic clay (w_L = 78–85%; I_P = 58–63%) reported by Kassiff and Shalom (1971), where the type of stress paths during swelling-pressure tests predicted by the framework is again obtained (Fig. 24).

The stress paths plotted in Fig. 22 indicate that for near-saturated conditions the swelling pressure will tend towards

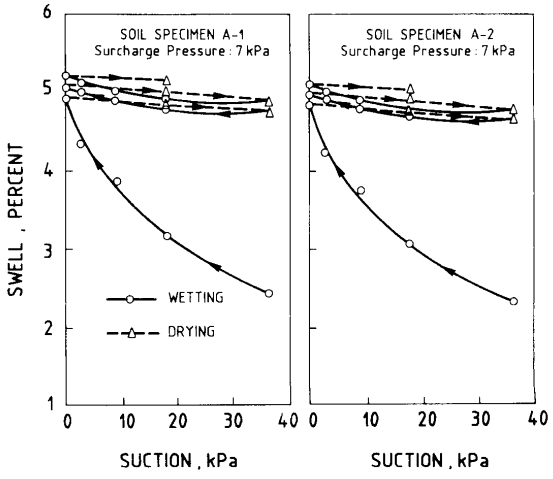

FIG. 19. Relationship between suction and swelling determined by controlled suction tests (after Chu and Mou 1973).

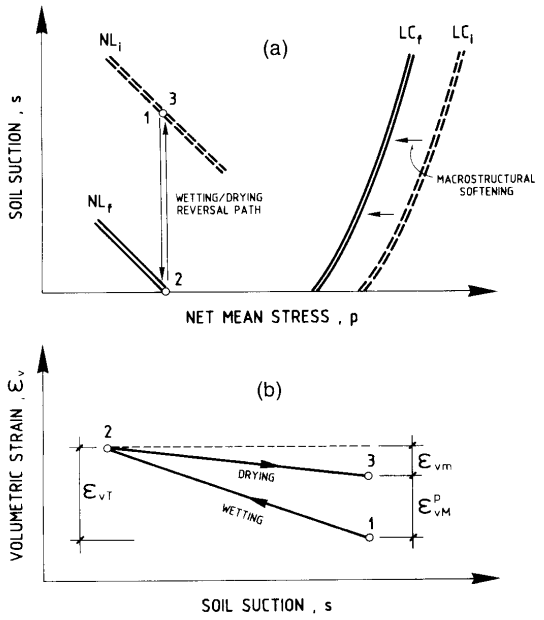

FIG. 20. Irreversible swelling strain in a wetting–drying cycle. (*a*) Stress paths. (*b*) Swelling strains.

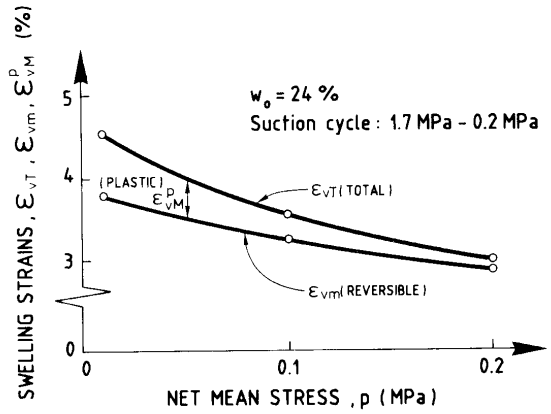

FIG. 21. Total, reversible, and irreversible strains in first wetting of compacted Madrid expansive clay (derived from tests by Pousada 1984).

the initial value of the suction. The smaller the degree of saturation, the larger the difference between initial suction and swelling pressure. As a result the swelling-pressure paths tend to converge towards a reduced zone along the p axis. This may explain in part the lack of correlation found between initial water content and swelling pressures (Shanker *et al.* 1982; Sridharan *et al.* 1986; Brackley 1973; Chen 1973). These authors, among others, find that swelling pressure is primarily related to initial void ratio.

The same convergence of swelling pressures of samples with the same density but different initial suctions (or water

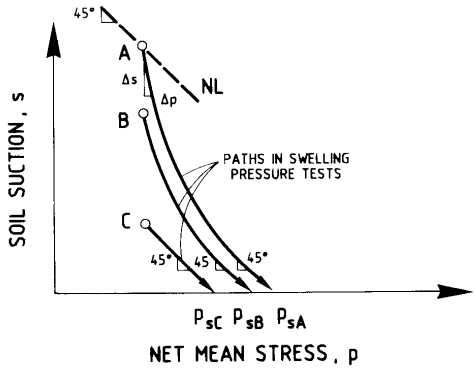

FIG. 22. Stress paths during constant-volume wetting from different initial suctions.

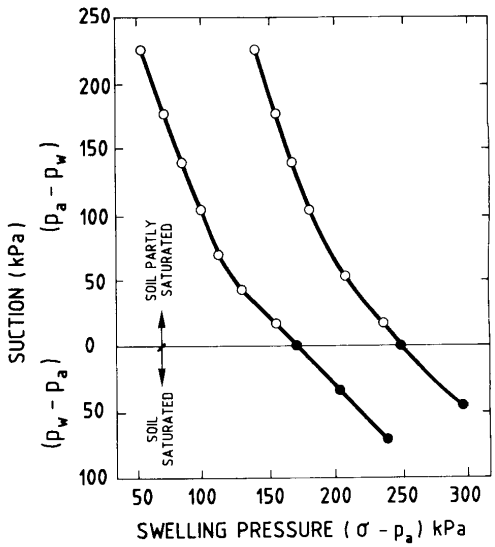

FIG. 23. Typical swelling-pressure stress paths for an unsaturated expansive clay (after Blight 1965).

content) is predicted when the stress paths during the tests reach the LC yield surface (Fig. 25). Different samples such as A or B at the same macrostructural void ratio are characterized by a common loading–collapse yield function. Saturation paths under constant volume (A → A′; B → B′) may bring the stress state of both samples to the LC yield locus. The collapse tendency experienced by the macrostructure of both samples at A′ and B′ has to be compensated by a decrease in confining pressure. In fact, if collapse strains tend to dominate in magnitude other contributions to the total volumetric deformation, the stress path will follow closely the LC_i yield locus as indicated in Fig. 25. In the case of sample A, the reduction in macrostructural pore space (compensated by a expansion of the microstructure) leads to the final position (LC_f) indicated for the loading–collapse yield function. The swelling pressures p_{sB} and p_{sA} will not in general differ much from the yield stress for

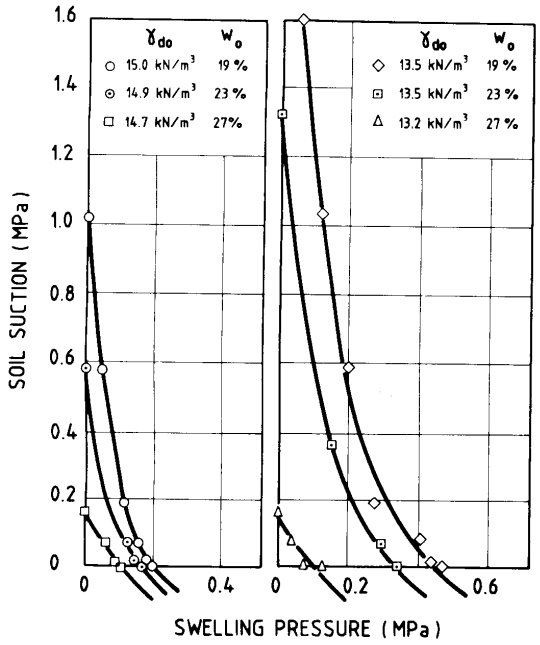

FIG. 24. Swelling-pressure stress paths at two dry densities for a calcium montmorillonite clay (after Kassiff and Shalom 1971).

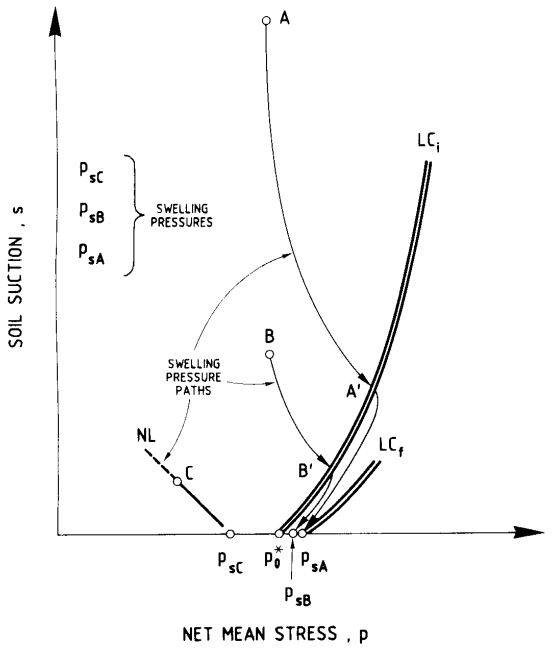

FIG. 25. Constant-volume stress paths during wetting affected by the loading-collapse yield curve.

saturated conditions p_0^*. As a result, irrespective of their initial water contents, samples A and B will tend to show a common swelling pressure.

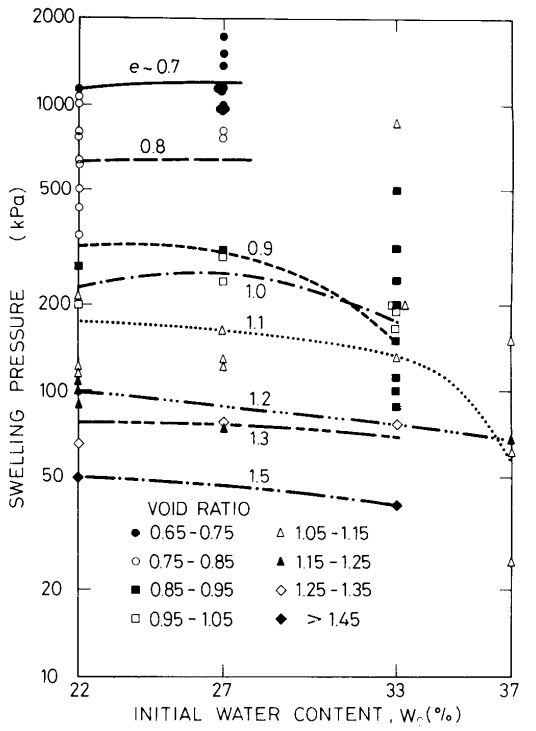

FIG. 26. Constant-volume swelling pressures of a compacted, high-plasticity clay plotted in terms of initial water contents and void ratio (from data published by Brackley 1973).

According to the model, however, there will be situations not leading to a common swelling pressure. They are exemplified by sample C, which is again supposed to have the same LC_i yield locus and therefore the same macrostructural void ratio. However, its water content is higher, and hence its suction is significantly lower. According to previous reasoning, the stress path for zero volume change will closely follow the neutral line through C, NL. It is now more likely that this swelling path will reach the p axis at a value $p_{sC} < p_0^*$. In fact, the lower the initial suction (i.e., the higher the initial water content), the greater are the chances of finding swelling pressures smaller than the common value for the given initial void ratio. Brackley (1973) published the results of a large number of swelling-pressure tests on dynamically compacted samples of high-plasticity weathered norite (w_L = 89%; I_P = 57%) at different initial void ratios and water contents which are relevant to this discussion. The results (Fig. 5 of his paper) demonstrated that swelling pressure was essentially related to void ratio. However, a reduction in swelling pressure was noticed for samples compacted at the higher water contents. The results provided by Brackley have been represented in Fig. 26 using different axes. Swelling pressure has been plotted in terms of water content for different ranges of void ratio. Despite the scatter, Fig. 26 shows that at higher water contents there is a trend towards a decrease in swelling pressure. This corresponds to model predictions, but certainly more

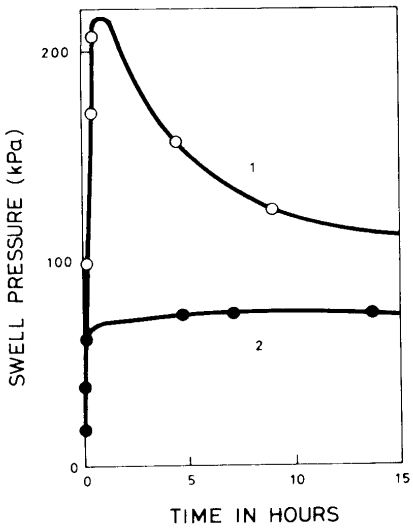

FIG. 27. Swell pressure vs. time relationship for a compacted, high-plasticity clay (after Brackley 1973).

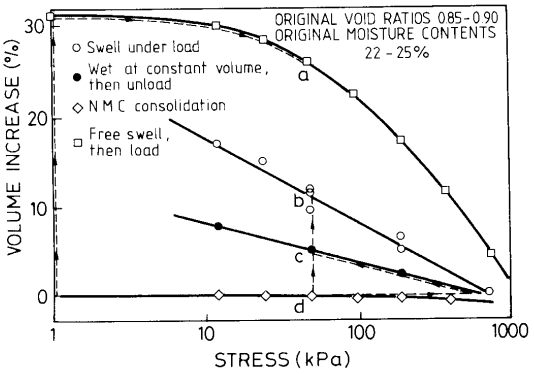

FIG. 28. Procedures for swell prediction (after Brackley 1975*a*). NMC, natural moisture content.

experimental evidence is necessary to firmly establish the validity of these results.

The stress paths for samples such as A or B in Fig. 25 imply that the swelling pressure may reach a maximum at some intermediate stage during the wetting process. This will be particularly so the higher the initial suction. Samples with a relatively high initial water content will, on the contrary, exhibit a continuous increase in swelling pressure during wetting. This would be the case for sample C in Fig. 25. Results showing this behaviour were published by Brackley (1973) (see Fig. 27) for the soil already described in connection with Fig. 26. Sample 1 in Fig. 26 had the following original properties: e_o = 1.17, s_o = 60 000 kPa, and w_o = 12%; whereas sample 2 had e_o = 1.46, s_o = 1100 kPa, and w_o = 30%. These characteristics are, according to the previous qualitative discussion, in agreement with the measured evolution of swelling pressure.

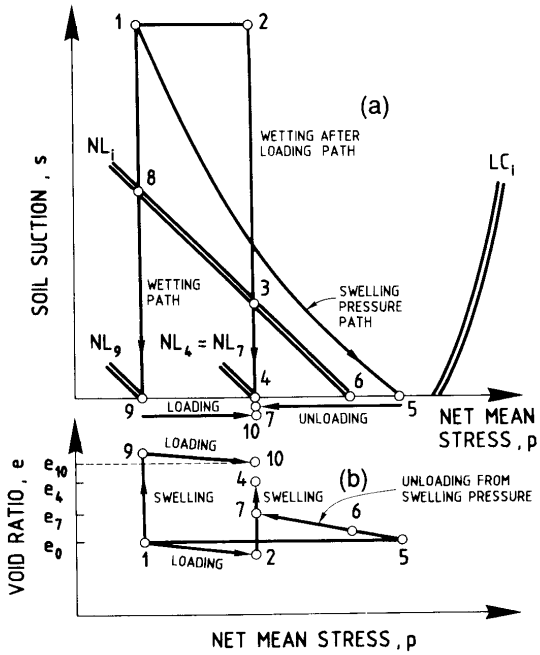

FIG. 29. Alternative procedure to obtain swelling volumetric deformation upon wetting for a given confining stress. (*a*) Stress path. (*b*) Predicted volumetric response.

Stress-path dependency of swelling deformation and swelling pressure

The stress-path dependency of swelling strains and swelling pressures exhibited by expansive clays have long been recognized and will provide a final illustration of the performance of the model. Stress-path dependency of swelling deformations is exemplified by the test results of Fig. 28 reported by Brackley (1975*a*), where three techniques to predict heave under a given load of 50 kPa are considered: (*i*) free swell and subsequent loading, (*ii*) loading to 50 kPa and swell under pressure, and (*iii*) saturation at constant volume and subsequent unloading to 50 kPa. The first method yields the maximum swelling (interval *d*–*a* in Fig. 28), the third method gives the smallest deformation (segment *d*–*c*), and the second method results in an intermediate swelling value (segment *d*–*b*).

The tests are interpreted in terms of the framework in Fig. 29. The initial state of the soil is defined by yield locus LC_i and neutral line NL_i. Procedure *i* (free swell under small token load followed by loading) is represented by stress path 1–8–9–10. It can be observed that the stage of irreversible expansion (8–9) takes place at the maximum distance of the yield locus, and therefore plastic swelling strains will be the largest in this case. Stress path 1–2–3–4 corresponds to method *ii* (loading to specified stress and subsequent saturation). There is also a stage of irreversible swelling (3–4), but it occurs closer to the LC yield surface, and therefore the final swelling strains will also be smaller. Finally, procedure *iii* results in the stress path 1–5–6–7. Stress path 1–5 corresponds to the swelling under constant volume

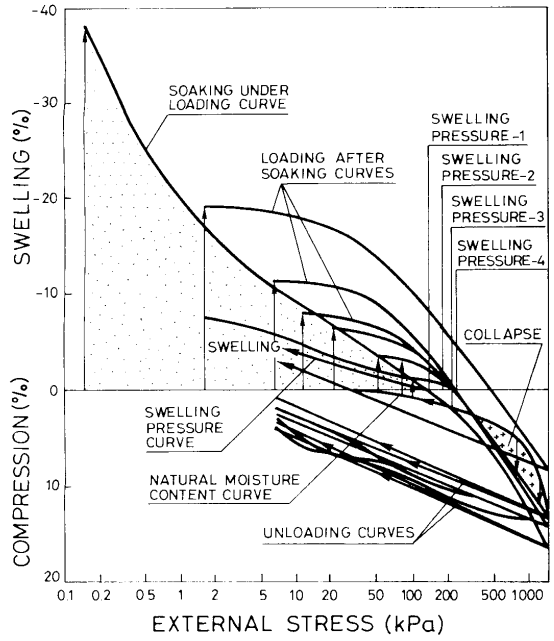

FIG. 30. Soaking tests on compacted samples of El Arahal (after Justo *et al.* 1984).

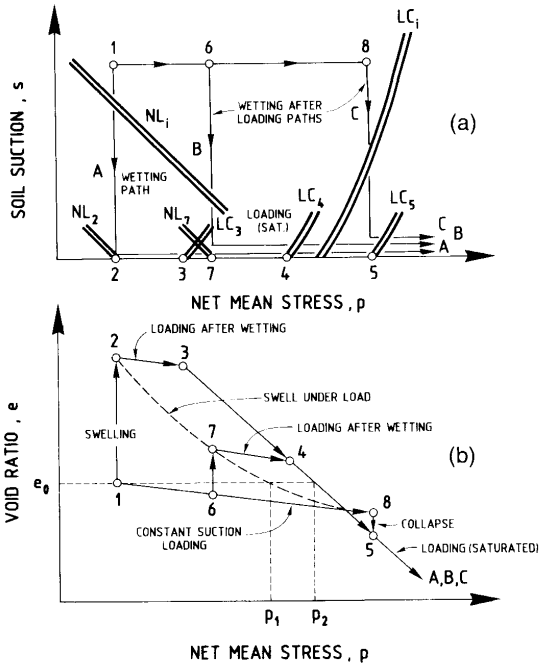

FIG. 31. Swelling-pressure tests. (*a*) Stress paths in a (p, s) stress space. (*b*) Predicted volumetric response.

stage, whereas the subsequent unloading is represented by 5–6–7. It can be noted that now the irreversible swelling stage (6–4) occurs closer to the LC yield locus than in any of the other cases and, therefore, final swelling strains will be the smallest. Although the microstructural swelling strains are considered in this simple model independent of stress path, stress-path dependency is accounted for in a natural way by the postulated interaction between microstructure and macrostructure.

Stress-path dependency of soil expansion also affects the determination of swelling pressures. As mentioned before, several alternative methods of carrying out swelling-pressure tests have been proposed. In addition to the zero volume change procedure discussed in the previous section, two other methods seem to be in practical use. One of them involves the initial wetting of the sample under some (small) load and its subsequent loading to recover the initial void ratio. The second method requires the testing of several samples. Each one of them is first loaded to a different value of vertical stress and, once consolidated, allowed to swell (or collapse) during the wetting process at constant applied stress. The final equilibrium positions of the samples describe a "swell under load" curve, which defines a swelling pressure corresponding to a load equal to the original void ratio. These procedures may be followed in Fig. 30 taken from Justo *et al.* (1984). The first method is consistently reported to give a higher value of swelling pressure than the second method. The constant-volume method gives pressures that have been reported to be intermediate between the preceding two methods (Justo *et al.* 1984; Sridharan *et al.* 1986) or to yield the lowest values (El-Sohby *et al.* 1989).

This behaviour is a consequence of the stress-path dependency observed in the behaviour of expansive and, more generally, unsaturated soils. These effects may be conveniently analyzed within the developed framework. Consider in Fig. 31*a* a sample of expansive soil defined by the initial values of its loading–collapse yield curve LC_i and its neutral line $N L_i$. Three alternative stress paths, A, B, and C, have been plotted in Fig. 31*a*. The response of the soil to these three sequences of wetting and loading is qualitatively shown in Fig. 31*b*. Path A (1 → 2 → 3 → 5) describes the "free swelling and loading" method to obtain the swelling pressure. Under the first wetting (1 → 2) reversible and irreversible swelling deformations take place. The neutral line reaches the position $N L_2$, and as a result of the plastic components of swelling, the LC_i yield locus moves back to position LC_3. Upon loading (path 2→ 3), sample A begins to yield at a stress p_3 lower than the original yield stress under saturated conditions, p_0^*. Under further loading (3 → 5 →) a virgin saturated consolidation curve is obtained.

Path B (6 → 7) involves a smaller development of plastic swelling. As a consequence LC_i moves backward to a position LC_4 intermediate between LC_i and LC_3. When loaded after saturation, sample B yields at p_4^* on the virgin consolidation line. Further loading follows the saturated virgin line. Under path C it is assumed that the sample is loaded, at constant suction, up to a pressure (point 8) that leads to collapse upon saturation (8 → 5). Two of the usual "swelling pressures" definitions p_1 and p_2 may be obtained in Fig. 31*b*. Pressure p_2 (free swell and loading method) is in fact larger than pressure p_1 (swell under load method) which is consistent with most experimental observations.

Note that points 3, 4, and 5 in Fig. 31*b* are all of the same virgin consolidation line and that, upon subsequent loading, they follow the saturated consolidation line. This is a consequence of one of the hypotheses of the model which specifies that the position of the LC yield curve is uniquely controlled by the plastic volumetric macrostructural deformations independently of their origin. It can be remarked that, with the exception of one test, this predicted convergence of consolidation lines after yield is observed in the results of the tests plotted in Fig. 30.

Shear strength

To the authors' knowledge, no comprehensive suction-controlled experimental programme has been performed to explore systematically the effect of shear stress q on the behaviour of unsaturated expansive clays. Regarding shear strength, Escario and Sáez (1986) have reported suction-controlled shear-box tests performed on expansive Madrid grey clay. They found that the dependence of shear strength on applied net stress and on suction is similar to that found in other nonexpansive materials, and therefore the expansive clay does not exhibit any special features in this respect. Further tests reported by Escario and Jucá (1989) performed over a much wider range of suctions confirm the similarity of behaviour of all these materials. Hence, the extended framework will account for the increase of the shear strength with suction in the same way as in the original formulation, i.e., through the variation of the critical state line with suction (Fig. 4). Therefore, and until more evidence becomes available, existing experimental results do not warrant a modification of the original framework in this respect.

Concluding remarks

The behaviour of unsaturated expansive clays can be best understood by considering the interaction between a capillary-controlled macrostructure and a microstructure where physicochemical and other phenomena occurring at particle level take place. A framework has been proposed which takes explicitly into account these two levels of structure. In this way the basic microstructural behaviour characteristics of expansive minerals and the models developed for unsaturated soils of low activity can be integrated in a single coherent whole.

The relationship between the two structural levels is defined in a simple way. Despite this, the framework is able to represent satisfactorily a number of important features of unsaturated expansive soil behaviour, i.e., dependence of swelling on moisture content, dry density, and applied pressure; strong dependency of swelling pressure on void ratio; irreversibility and stress-path dependency of swelling strains; and dependence of swelling pressures on testing method. In fact, the distinction between two structural levels provides the basis for a powerful general approach that can be extended to account for the pattern of swelling strain development with time as shown in Alonso *et al.* (1989, 1991).

It should be stressed that in this first proposal of the framework, simplicity in the assumptions adopted has been a fundamental criterion of choice. In this way, it is hoped that the basic features of both the formulation and the unsaturated expansive soil behaviour will stand out more clearly at the possible cost of a smaller degree of predictive capability of the model. Despite this, the qualitative agreement between predictions and experimental results is very encouraging.

One of the benefits of developing a theoretical framework is that experimental programmes can be devised to examine the hypotheses and main predictions of the model in a systematic manner. As a consequence, it is likely that as further and more comprehensive experimental data become available more complex versions of the framework will have to be used. It is thought, however, that the basic principles of the formulation put forward in this paper will be able to accommodate those future developments.

Acknowledgements

The support provided by the Dirección General de Política Científica y Técnica through Research grants PB86-0379 and PB90-0595 is gratefully acknowledged.

Alonso, E.E., Gens, A., and Hight, D.W. 1987. Special problem soils. General report. Proceedings, 9th European Conference on Soil Mechanics and Foundation Engineering, Dublin, vol. 3, pp. 1087–1146.

Alonso, E.E., Lloret, A., Gens, A., and Battle, F. 1989. A new approach for the prediction of long term heave. Proceedings, 12th International Conference on Soil Mechanics and Foundation Engineering, Rio de Janeiro, vol. 1, pp. 571–574.

Alonso, E.E., Gens, A., and Josa, A. 1990. A constitutive model for partially saturated soils. Géotechnique, **40**: 405–430.

Alonso, E.E., Gens, A., and Lloret, A. 1991. Double structure model for the prediction of longterm movements in expansive materials. Proceedings, 7th International Conference on Computer Methods and Advances in Geomechanics, Cairns, vol. 1, pp. 541–548.

Atabek, R.B., Felix, B., Robinet, J.-C., and Lahlou, R. 1991. Rheological behaviour of saturated expansive clay materials. Workshop on Stress Partitioning in Engineered Clay Barriers, Duke University, Durham, N.C.

Baveye, P., Verbug, K., and Bielders, C. 1991. Capillary phenomena and clay swelling. Proceedings, NATO Advanced Research Workshop on Clay Swelling and Expansive Soils, Cornell University, Ithaca, N.Y. In press.

Blight, G.E. 1965. The time-rate of heave of structures on expansive clays. *In* Moisture equilibria and moisture changes in soils beneath covered areas. *Edited by* G.D. Aitchison. Butterworths, Sydney. pp. 78–87.

Bolt, G.H. 1956. Physico-chemical analysis of the compressibility of pure clays. Géotechnique, **6**: 86–93.

Bolt, G.H., and Miller, R.D. 1955. Compression studies of illite suspensions. Soil Science Society of America Proceedings, **19**: 285–288.

Brackley, I.J. 1973. Swell pressure and free swell in compacted clay. Proceedings, 3rd International Conference on Expansive Soils, Haifa, vol. 1, pp. 169–176.

Brackley, I.J. 1975*a*. Swell under load. Proceedings, 6th Regional Conference for Africa on Soil Mechanics and Foundation Engineering, Durban, vol. 1, pp. 65–70.

Brackley, I.J. 1975*b*. A model for unsaturated clay structure and its application to swell behaviour. Proceedings, 6th Regional Conference for Africa on Soil Mechanics and Foundation Engineering, vol. 1, pp. 71–79.

Branson, K., and Newman, A.C.D. 1983. Water sorption on Ca-saturated clays: I. Multilayer sorption and microporosity in some illites. Clay Minerals, **18**: 277–287.

Callaghan, I.C., and Ottewill, R.H. 1974. Interparticle forces in montmorillonite gels. Faraday Discussions of the Chemical Society, **57**: 110–118.

Champan, D.L. 1913. A contribution to the theory of electrocapillarity. Philosophical Magazine, **25**: 475–481.

Chen, F.H. 1973. The basic physical property of expansive soils. Proceedings, 3rd International Conference on Expansive soils, Haifa, vol. 1, pp. 17–25.

Chu, T.Y., and Mou, C.H. 1973. Volume change characteristics of expansive soils determined by controlled suction test. Proceedings, 3rd International Conference on Expansive Soils, Haifa, vol. 1, pp. 177–185.

Collins, K. 1984. Characterisation of expansive soil microfabric. Proceedings, 5th International Conference on Expansive Soils, Adelaide, pp. 37–43.

Collins, K., and McGown, A. 1974. The form and function of microfabric features in a variety of natural soils. Géotechnique, **24**: 223–254.

Croney, D., Coleman, J.D., and Black, W.P.M. 1958. Studies of the movement and distribution of water in soil in relation to highway design and performance. Highway Research Board Special Report 40, pp. 226–252.

Delage, P., and Lefebvre, G. 1984. Study of the structure of a sensitive Champlain clay and of its evolution during consolidation. Canadian Geotechnical Journal, **21**: 21–35.

Delage, P., Tessier, D., and Marcel-Audiguier, M. 1982. Use of the cryoscan apparatus for observation of freeze-fractured planes of a sensitive Quebec clay in scanning electron microscopy. Canadian Geotechnical Journal, **19**: 111–114.

El-Sohby, M.A., Mazen, S.O., and Abon-Taha, M.M. 1989. Effect of apparatus deformability on swelling pressure. Proceedings, 12th International Conference on Soil Mechanics and Foundation Engineering, Rio de Janeiro, vol. 1, pp. 589–592.

Escario, V., and Jucá, J.F.T. 1989. Strength and deformation of partly saturated soils. Proceedings, 12th International Conference on Soil Mechanics and Foundation Engineering, Rio de Janeiro, vol. 1, pp. 43–46.

Escario, V., and Sáez, J. 1986. The shear strength of partly saturated soils. Géotechnique, **36**: 453–456.

Fredlund, D.G., and Morgenstern, N.R. 1977. Stress rate variables for unsaturated soils. ASCE Journal of the Geotechnical Engineering Division, **103**(GT5): 261–276.

Gens, A., Alonso, E.E., and Josa, A. 1979. Elastoplastic modelling of partially saturated soils. Proceedings, 3rd International Symposium on Numerical Models in Geomechanics, Niagara Falls, pp. 163–170.

Gouy, G. 1910. Sur la constitution de la charge électrique à la surface d'un électrolyte. Physique, **9**: 457–468.

Gouy, G. 1917. Sur la fonction électrocapilaire, Annales de Physique (Paris), Série 9, **7**: 129–184.

Graham, J., Oswell, J.M., and Gray, M.N. 1992. The effective stress concept in saturated sand–clay buffer. Canadian Geotechnical Journal, **29**: 1033–1043.

Jadayeva, M.S., and Sridharan, A. 1982. A study on potential distance relationship of clays. Indian Geotechnical Journal, **12**: 83–97.

Josa, A., Alonso, E.E., Lloret, A., and Gens, A. 1987. Stress–strain behaviour of partially saturated soils. Proceedings, 9th European Conference on Soil Mechanics and Foundation Engineering, Dublin, vol. 2, pp. 561–564.

Juang, C.H., and Holtz, R.D. 1986. Fabric, pore size distribution and permeability of sandy soils. ASCE Journal of Geotechnial Engineering, **112**(GT9): 855–868.

Justo, J.L., Delgado, A., and Ruiz, J. 1984. The influence of stress-path in the collapse-swelling of soils at the laboratory. Proceedings, 5th International Conference on Expansive Soils, Adelaide, pp. 67–71.

Kassiff, G., and Shalom, A.B. 1971. Experimental relationship between swell pressure and suction. Géotechnique, **21**: 249–255.

Kassiff, G., Baker, R., and Ovadia, Y. 1973. Swell-pressure relationships at constant suction changes. Proceedings, 3rd International Conference on Expansive Soils, Haifa, vol. 1, pp. 201–208.

Kjellander, R. 1991. Electrostatic ion–ion correlation forces, a possible mechanism for restricted calcium-clay swelling. Proceedings, NATO Advanced Research Workshop on Clay Swelling and Expansive Soils, Cornell University, Ithaca, N.Y. In press.

Kraehenbuehl, F., Stoeckli, M.F., Brunner, F., Kahr, G., and Müller-Vonmoos, M. 1987. Study of the water–bentonite system by vapour adsorption, immersion calorimetry and X-ray technique: I. Micropore volumes and internal surface areas, following Dubinin's theory. Clay Minerals, **22**: 1–9.

Lapierre, C., Leroueil, S., and Locat, J. 1990. Mercury intrusion and permeability of Louisville clay. Canadian Geotechnical Journal, **27**: 761–773.

Low, P.F. 1980. The swelling of clay. II. Montmorillonites. Soil Science Society of America Journal, **44**: 667–676.

Low, P.F. 1991. Structural and other forces involved in the swelling of clays. Proceedings, NATO Advanced Research Workshop on Clay Swelling and Expansive Soils, Cornell University, Ithaca, N.Y. In press.

Low, P.F., and Margheim, J.F. 1979. The swelling of clay. I. Basic concepts and empirical equations. Soil Science Society of America Journal, **43**: 473–481.

Madsen, F.T., and Müller-Vonmoos, M. 1985. Swelling pressure calculated from mineralogical properties of a Jurassic opalinum shale, Switzerland. Clays and clay minerals, **33**: 501–509.

McGown, A., and Collins, K. 1975. The microfabrics of some expansive and collapsing soils. Proceedings, 5th Pan-American Conference on Soil Mechanics and Foundation Engineering, Buenos Aires, vol. 1, pp. 323–332.

Mitchell, J.K. 1976. Fundamentals of soil behaviour. John Wiley & Sons, Inc., New York.

Olson, R.E., and Mesri, G. 1970. Mechanisms controlling the compressibility of clay. ASCE Journal of the Soil Mechanics and Foundations Division, **96**(SM6): 1863–1878.

Ormerod, E.C., and Newman, A.C.D. 1983. Water sorption of Ca-saturated clays: II. Internal and external surfaces of montmorillonite. Clay minerals, **18**: 289–299.

Pousada, E. 1984. Deformabilidad de arcillas expansivas bajo succíon controlada. Doctoral thesis, Universidad Politénica de Madrid, Spain.

Pusch, R. 1970. Microstructural changes in soft quick clay at failure. Canadian Geotechnical Journal, **7**: 1–7.

Pusch, R. 1973. Influence of salinity and organic matter on the formation of clay microstructure. Proceedings of International Symposium on Soil Stucture, Gothenburg, pp. 161–173.

Pusch, R. 1982. Mineral–water interactions and their influence on the physical behaviour of highly compacted Na bentonite. Canadian Geotechnical Journal, **19**: 381–387.

Shanker, N.B., Rao, A.S., and Swamy, A.S.R. 1982. Swelling behaviour of undisturbed and remoulded samples of black cotton clay. Indian Geotechnical Journal, **12**: 152–159.

Smart, P. 1973. Structure of red clay soil from Nyeri, Kenya. Quarterly Journal of Engineering Geology, **6**: 129–139.

Sridharan, A., and Jayadeva, M.S. 1982. Double layer theory and compressibility of clays. Géotechnique, **32**: 133–144.

Sridharan, A., and Rao, G.V. 1973. Mechanisms controlling volume change of saturated clays and the role of the effective stress concept. Géotechnique, **23**: 359–382.

Sridharan, A., Rao, A.S., and Sivapullaiah, P.V. 1986. Swelling pressure of clays. Geotechnical Testing Journal, **9**: 24–33.

Sridharan, A., Altschaeffl, A.G., and Diamond, S. 1971. Pore size distribution studies. Journal of the Soil Mechanics and Foundations Division, **97**(SM5): 771–787.

Tessier, D. 1991. Electron microscope studies of clay microstructures. Proceedings, NATO Advanced Research Workshop on Clay Swelling and Expansive Soils, Cornell University, Ithaca, N.Y. In press.

Vicol, T. 1990. Comportement hydraulique et mécanique d'un sol fin non saturé. Application à la modélisation, Thèse de doctorat, École Nationale des Ponts et Chaussées, Paris.

Wan, A.W.L., Graham, J., and Gray, M.N. 1990. Influence of soil structure on the stress–strain behavior of sand–bentonite mixtures. Geotechnical Testing Journal, **13**: 179–187.

Warkentin, B.P., Bolt, G.M., and Miller, R.D. 1957. Swelling pressure of montmorillonite. Soil Science Society of America Proceedings, **21**: 495–497.

Yong, R.N., and Sheeran, D.E. 1973. Fabric unit interaction and soil behaviour. Proceedings of International Symposium on Soil Structures, Gothenburg, pp. 176–183.

Yong, R.N., Japp, R.D., and How, G. 1971. Shear strength of partially saturated clays. Proceedings, 4th Asian Regional Conference on Soil Mechanics and Foundations Engineering, Bangkok, vol. 2, pp. 183–187.

Yong, R.N., Sadana, M.L., and Gohl. W.B. 1984. A particle interaction model for assessment of swelling of an expansive soil. Proceedings, 5th International Conference on Expansive Soils, Adelaide, pp. 4–12.

List of Symbols

e	void ratio
I_P	plasticity index
p	net mean stress (excess of mean stress over air pressure)
p_a	air pressure
p_o	net mean yield stress at current suction
p_o^*	net mean yield stress at zero suction
p_s	swelling pressure
p_w	water pressure
q	deviatoric stress ($= \sigma_1 - \sigma_3$)
s	suction ($= p_a - p_w$)
S_{ro}	initial degree of saturation
v	specific volume ($= 1 + e$)
w	water content
w_L	liquid limit
w_P	plastic limit
γ_d	dry unit weight
δ_{ij}	Kronecker's delta
ϵ_m	microstructural strain
ϵ_M	macrostructural strain
ϵ_T	total strain
ϵ_{vm}	microstructural volumetric strain
ϵ_{vM}	macrostructural volumetric strain
ϵ_{vM}^P	irreversible macrostructural volumetric strain
ϵ_{vT}	total volumetric strain
σ_{ij}	total stresses
σ_v	total vertical stress
σ_1, σ_3	major and minor principal stresses